Recent Progress of MgB_2 Bulk Magnets Magnetized by Pulsed Field

Hiroyuki Fujishiro, Toru Ujiie, Hidehiko Mochizuki, Takafumi Yoshida, and Tomoyuki Naito

***Abstract*—A MgB_2 superconducting bulk has a promising potential as a quasi-permanent magnet. In this paper, we have performed pulsed-field magnetization (PFM) at $T_s = 14$–20 K for MgB_2 superconducting bulks with a higher critical current density $J_c(B)$ fabricated by hot isostatic pressing. During PFM, a flux jump frequently took place, and trapped field B_z decreased in the disk-shaped bulks for a higher magnetic field application. However, in the cylindrical bulk with identical $J_c(B)$ characteristics, the flux jump was avoided, and a maximum trapped field of $B_z = 0.81$ T was obtained at 14 K, which is a record-high trapped field in a MgB_2 bulk by PFM. The electromagnetic and thermal instability was discussed using conventional relations to avoid the flux jump and to enhance the trapped field on the MgB_2 bulks with higher $J_c(B)$, higher thermal conductivity, and lower specific heat.**

***Index Terms*—Critical current density, flux jump, MgB_2 bulk magnet, pulsed-field magnetization (PFM), thermal and electromagnetic stability.**

I. Introduction

SUPERCONDUCTING bulk magnets using REBaCuO (RE: rare earth element or Y) are one of the typical candidates for practical applications such as sputtering cathodes, magnetic separation and drug delivery systems (DDSs), which can result in tesla-order quasi-permanent magnets [1]. However, it is difficult to fabricate a large single-domain bulk with good, homogeneous superconducting properties over 100 mm in diameter. MgB_2 superconducting bulk has also a promising potential as a quasi-permanent magnet, which has a number of attractive properties, such as low-cost, light-weight and homogeneous trapped field distribution, which are in clear contrast with the REBaCuO bulk magnet. The problem of weak-links at grain boundaries can be ignored in the MgB_2 polycrystalline bulk due to their long coherence length, ξ [2]. These characteristics enable us to realize better and larger polycrystalline MgB_2 bulk magnets below the transition temperature $T_c = 39$ K, which are expected to be applicable in magnetically levitated trains (MAGLEVs) and wind power generators using liquid H_2 or cryocooler system. Several groups have already reported the trapped field for MgB_2 bulks activated by the field-cooled magnetization (FCM). The trapped field B_z was reported to be 2.25 T at 15 K on the single MgB_2 bulk disk [3] and 3.14 T at 17.4 K in the disk pair [4]. We have attained 3.6 T and 4.6 T at 14 K in single and paired disks of Ti-doped MgB_2 bulks 35 mm in diameter fabricated by a hot isostatic pressing (HIP) method [5]. Recently, a record-high trapped field of 5.4 T has been attained at 12 K on the MgB_2 bulk 20 mm in diameter, which was fabricated by hot-pressing of ball-milled Mg and B powders using fine-grained boron powders [6].

Pulsed-field magnetization (PFM) has also been investigated to magnetize the bulk superconductors. However, for REBaCuO bulks, the trapped field B_z achievable by PFM is nonetheless lower than that achievable by FCM because of a large temperature rise caused by the dynamic motion of the magnetic flux. Several approaches using the multi-pulse techniques have been reported to be effective to reduce the temperature rise and then to enhance B_z [7], [8]. We have also investigated the trapped field B_z and the temperature rise on the cryocooled REBaCuO bulks during PFM for various conditions [9]. We proposed a new PFM technique named a modified multi-pulse technique with stepwise cooling (MMPSC) and successfully realized the highest trapped field of $B_z = 5.20$ T on a GdBaCuO bulk with 45 mm in diameter at 30 K [10], which is a record-high value magnetized by PFM to date. For the MgB_2 bulk, we have performed the PFM to the bulk fabricated by various methods. $B_z = 0.41$ T was achieved at 14 K for the bulk ($B_z(\mathrm{FCM}) = 1.4$ T at 20 K) fabricated by a reactive liquid Mg infiltration (Mg-RLI) method [11]. $B_z = 0.71$ T was also obtained at 14 K for the bulk ($B_z(\mathrm{FCM}) = 1.5$ T at 14 K) fabricated by a capsule method [12]. Considering the experimental results and theoretical estimation for the REBaCuO system, the $B_z(\mathrm{PFM})$ value for the MgB_2 bulk is expected to be enhanced by using the bulk with higher $B_z(\mathrm{FCM})$ value and higher critical current density J_c. Homogeneity is also very important from studies on REBaCuO bulks and we should add this as a factor for expected enhanced $B_z(\mathrm{PFM})$ values.

In this study, we applied the PFM technique to the MgB_2 bulks with higher J_c values fabricated by a hot isostatic pressing (HIP) method. For the MgB_2 bulk during PFM, flux dynamics and heat generation are supposed to be in clear contrast with those in the REBaCuO bulk because of a small specific heat, large thermal conductivity, and narrow temperature margin against T_c. The electromagnetic and thermal stability in the MgB_2 bulk during PFM was discussed.

II. Experimental Procedure

Three MgB_2 superconducting bulks (hereafter, HIP#38, HIP-Ti20% and HIP#22) were fabricated by a HIP method [5]. The

Manuscript received August 3, 2014; accepted September 15, 2014. Date of publication September 19, 2014; date of current version January 13, 2015. This work was supported in part by the Grant-in-Aid for Scientific Research under Grant 23560002 from the Japanese Ministry of Education, Culture, Sports, Science, and Technology, and in part by the Japan Science and Technology Agency under the Adaptable and Seamless Technology Transfer Program through target-driven R&D for an Exploratory Research of FS stage under Grant AS242Z02673L.

The authors are with the Faculty of Engineering, Iwate University, Morioka 020-8551, Japan (e-mail: fujishiro@iwate-u.ac.jp).

Color versions of one or more of the figures in this paper are available online at http://ieeexplore.ieee.org.

Digital Object Identifier 10.1109/TASC.2014.2359544

TABLE I
SPECIFICATION OF THE MEASURED MgB_2 BULKS

Bulk name	HIP#38	HIP-Ti20%	HIP#22	CAP#30
Diameter d (mm)	38	36	22	30
Thickness t_B (mm)	7	7	18	10
Aspect ratio (d/t_B)	5.4	5.1	1.2	3.0
B_z^{max} by FCM at 16 K	2.38 T	3.30 T	2.23 T	1.50 T
Relative mass density	93%	94%	93%	50%

specification of the bulks and the maximum of the trapped field B_z^{max} by FCM are summarized in Table I. For the HIP#38 and HIP#22 bulks, a precursor pellet was prepared by cold isostatic pressing at 196 MPa using mixed powders of Mg (99.5% in purity, $\leqslant 180$ μm in grain size) and B (99% in purity, 300 mesh in grain size) with a molar ratio of 1.0: 2.0. For the HIP-Ti20% bulk, Mg, B, and Ti (99% in purity, ≤ 45 μm in grain size) powders were mixed with a molar ratio of Mg:B:Ti $= 0.8 : 2.0 : 0.2$ and the precursor pellet was fabricated. These pellets were sealed under vacuum in a stainless steel container and were heated at 900 °C for 3 h under an isostatic pressure of 98 MPa. For comparison, the CAP#30 bulk fabricated by a capsule method, was investigated [12]–[14].

Each MgB_2 bulk was mounted in a stainless steel ring with a slightly larger inner diameter using epoxy resin (Stycast 2850). The outer diameter of the ring was fixed to be 65 mm for each bulk. The bulk was tightly anchored onto the cold stage of a Gifford–McMahon (GM) cycle helium refrigerator. The details of the PFM procedure were described elsewhere [9], [12]. The initial temperature T_s of the bulk was set at either 14 or 20 K. The magnetizing solenoidal copper magnetizing coil (99 mm I.D., 121 mm O.D., and 50 mm height), which was submersed in liquid nitrogen, was placed outside the vacuum chamber. A magnetic pulse B_{ex} up to 2.2 T with a rise time of 0.013 s and a duration of 0.15 s was applied via a pulse current in the coil. The time evolution of the local field $B_z^C(t)$ and the subsequent trapped field B_z at the bulk center were monitored by a Hall sensor (BHT 921; F W Bell), which was adhered to the center of the bulk surface. Two-dimensional trapped field profiles of B_z (1 mm) were mapped on the bulk at 1 mm above the bulk surface, scanned stepwise with a pitch of 1 mm by scanning an axial-type Hall sensor (BHA 921; F W Bell) using an $x-y$ stage controller. During PFM, the time evolution of the temperature $T(t)$ was also measured on the side surface of the ring using a thermometer (Cernox; Lakeshore).

III. RESULTS AND DISCUSSION

Fig. 1(a) and (b) show, respectively, the temperature dependence of the trapped field B_z for FCM (-0.222 T/min from 5 T), and the magnetic field dependence of the critical current density $J_c - B$ for each bulk. After the FCM experiment, the magnetization curves of several small pieces cut from the bulk were measured, and the $J_c - B$ characteristics were estimated using an extended Bean model [15]. The B_z values for the bulks fabricated by HIP are higher than that for the CAP#30 bulk [13], which are closely correlated with the $J_c - B$ characteristics shown in Fig. 1(b). In particular, the B_z value of the HIP-Ti20% bulk is the highest because of the highest $J_c - B$ characteristics due to the introduction of the strong pinning centers [5].

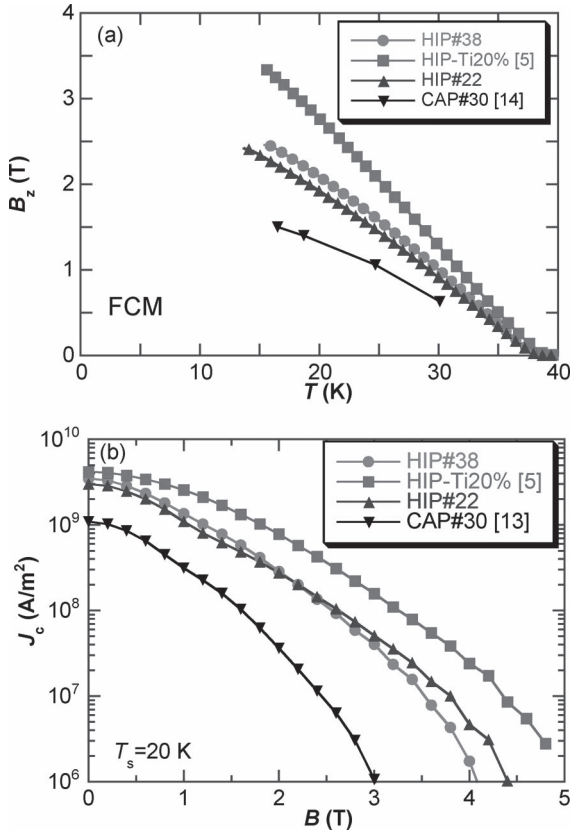

Fig. 1. (a) Temperature dependence of trapped field B_z on each bulk magnetized by FCM. (b) Magnetic field dependence of critical current density J_c for each bulk at $T_s = 20$ K.

Fig. 2(a) shows the relation between the trapped field B_z by PFM and the applied pulsed field B_{ex} for the HIP#38 bulk at $T_s = 14$ and 20 K. Similar to the previous experimental results for PFM of REBaCuO and MgB_2 bulks [9], [12], the B_z value increases, takes a maximum and then decreases with further increasing B_{ex}. The critical applied field B_{ex}^C, at which the magnetic flux starts to trap at the bulk center, increases with decreasing T_s due to the increase in J_c. However, for the bulk with higher J_c value, flux jump took place frequently for higher applied field.

Fig. 2(b) depicts an example of a flux jump; the time evolution of the local field $B_L^C(t)$ at the center surface of the HIP#38 bulk and applied pulsed field $B_{ex}(t)$ at $B_{ex} = 1.97$ T and at $T_s = 14$ K. $B_L^C(t)$ started to increase with a slight time delay, took a maximum at 0.016 s and then suddenly dropped about 40% at $t = 0.06$ s by the flux jump. Then, $B_L^C(t)$ approaches to the final value B_z due to flux flow. In the figure, the estimated $B_L^C(t)$ curve was also shown, in which no flux jump appears to take place during PFM. In Fig. 2(a), open circles and dotted lines show the estimated B_z values without a flux jump. If the flux jump can be avoided, the B_z value over 1 T can be realized at $T_s = 14$ K. The flux jump was always observed for HIP#38 and HIP-Ti20% bulks for pulsed fields higher than 1.5 T. The minimum applied pulsed field, at which the flux jump occurs, did not depend on T_s.

Fig. 3(a) and (b) present the trapped field profiles B_z (1 mm) of the HIP#38 bulk after applying pulsed field of $B_{ex} = 1.42$ T and 1.79 T at 14 K, respectively. For $B_{ex} = 1.42$ T, the profile

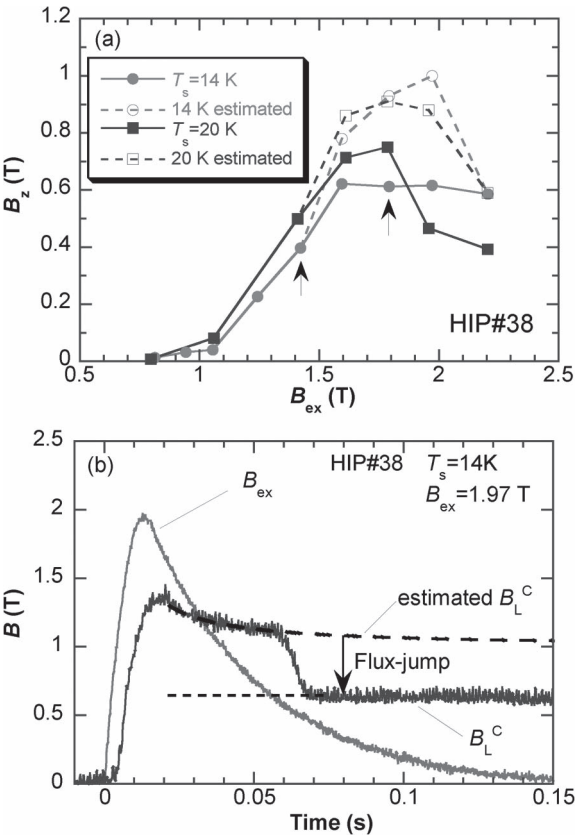

Fig. 2. (a) Applied pulsed-field dependence of trapped field B_z for the HIP#38 bulk at $T_s = 14$ and 20 K. The dashed lines show the estimated B_z value if no flux jump takes place during PFM (see text). (b) Time evolution of the local field $B_L^C(t)$ at the center of the HIP#38 bulk surface and pulsed field $B_{ex}(t)$ at $B_{ex} = 1.97$ T and at $T_s = 14$ K.

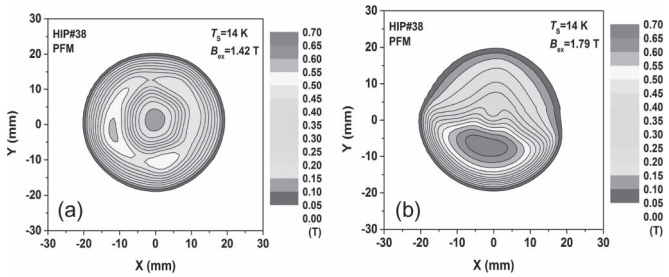

Fig. 3. Trapped field profiles B_z (1 mm) of the HIP#38 bulk after applying a pulsed field of (a) $B_{ex} = 1.42$ T and (b) 1.79 T at 14 K.

is concave and nearly concentric because of lower B_{ex}. On the other hand, for $B_{ex} = 1.79$ T as shown in Fig. 3(b), the profile is asymmetric and the magnetic flux in upper regions might escape due to flux jumps.

Fig. 4 shows the trapped field B_z for each bulk at $T_s = 14$ K as a function of applied pulsed field B_{ex}. In the figure, open and closed symbols show the B_z values with and without flux jumps, respectively. The magnetic flux easily penetrated into the CAP#30 bulk and was trapped at the center of the bulk with $B_z = 0.71$ T without flux jumps [12]. For the HIP#38 and HIP-Ti20% bulks, the magnetic flux starts to penetrate at higher B_{ex} than that for the CAP#30 bulk and was trapped in a similar manner. However, the B_z value for the HIP-Ti20% bulk with the highest J_c does not necessarily show the higher B_z value because of the flux escaping.

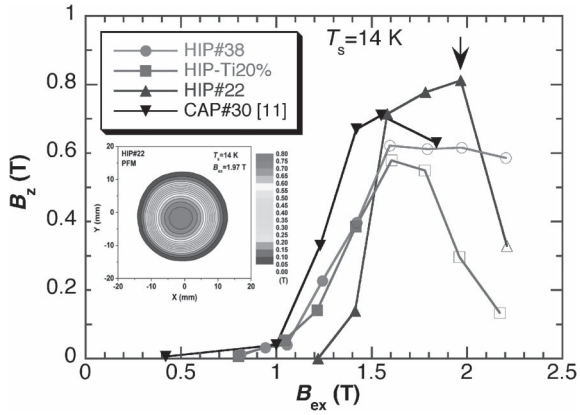

Fig. 4. Trapped field B_z by PFM for each bulk at $T_s = 14$ K as a function of the applied pulsed field B_{ex}.

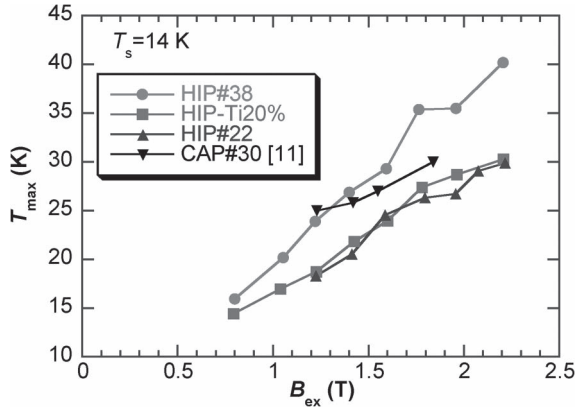

Fig. 5. Maximum temperature T_{max} during PFM for each bulk at $T_s = 14$ K as a function of the applied pulsed field.

On the other hand, the B_z-B_{ex} relation for the HIP#22 bulk is in clear contrast to those for other HIP bulks; the magnetic flux starts to penetrate at higher $B_{ex}^C (= 1.4$ T), B_z increases with increasing B_{ex} and takes a maximum of 0.81 T without flux jump at $B_{ex} = 1.97$ T. Then, B_z suddenly decreased for higher B_{ex} than 2 T due to the flux jump. $B_z = 0.81$ T is a record-high trapped field value by PFM for MgB_2 bulk to date. The inset shows the trapped field profiles B_z (1 mm) of the HIP#22 bulk at $B_{ex} = 1.97$ T. It should be noticed that the profile shows a conical profile, which is in clear contrast with other HIP bulks, even though the $J_c(B)$ and $B_z(\mathrm{FCM})$ of the HIP#22 bulk are nearly identical to those of the HIP#38 bulk. The significant feature of the HIP#22 bulk is a small aspect ratio (d/t_B); that is, the HIP#22 is cylindrical rather than disk-shaped. The result is not supported by the numerical simulation for FCM [16], where the B_z value slightly increases with increasing diameter (d) of the bulk, but is almost independent of the thickness (t_B). Increasing the t_B and d values is not necessarily an effective solution to enhance the B_z value. Since the travelling path of the magnetic flux along the radial direction in the HIP#22 bulk is shorter than that in the HIP#38 bulk, the heat generation is suppressed and flux jumps might be avoided.

Fig. 5 presents the maximum temperature T_{max} during PFM for each bulk at $T_s = 14$ K, as a function of applied pulsed field. The temperature rise for the HIP#22 bulk was the smallest, which supports the above discussion, even though the

TABLE II
PHYSICAL PARAMETERS AND ESTIMATED VALUES (l_m AND d_c) FOR MgB_2 AND GdBaCuO BULKS

Bulk name	HIP#38	HIP-Ti20%	CAP#30	GdBaCuO
T_c (K)	39	39	39	92
T_s (K)	20	20	20	40
κ (W/mK) at T_s	20	5.0	1.9	13
J_c (A/m^2) at T_s	1.3x10^9	2.6x10^9	3.1x10^8	2.7x10^9
ρ (Ωm) >T_c	2.1x10^{-8}	5.3x10^{-8}	1.1x10^{-7}	2.0x10^{-6}
γ (kg/m^3)	2.36x10^3	2.50x10^3	1.31x10^3	5.9x10^3
C (J/kgK) at T_s	2.9	3.6	2.9	62
l_m (μm) at T_s	146	23	82	10
d_c (mm) at T_s	0.86	0.48	2.66	4.9

temperature was measured indirectly on the side surface of the stainless steel ring. The results for the HIP#22 bulk may suggest an enhanced B_z and an avoidance of flux jumps by PFM and also by FCM.

We discuss the ease at which flux jumps occur and the magnetic instability during PFM using the conventional equations for superconducting wires. The minimum propagation zone (MPZ) l_m and the critical thickness d_c to avoid the flux jump from stability parameter can be written as follows [17],

$$l_m = \left\{ \frac{2\lambda(T_c - T_s)}{\rho J_c^2} \right\}^{\frac{1}{2}} \quad (1)$$

$$d_c = 2\sqrt{\frac{3\gamma C(T_c - T_s)}{\mu_0 J_c^2}}, \quad (2)$$

where T_c is the transition temperature and T_s is the operating temperature. κ, J_c, C, and γ are thermal conductivity, critical current density, specific heat and mass density at T_s, respectively. ρ is the normal state resistivity just above T_c. Table II shows these parameters and estimated l_m and d_c values for the HIP#38, HIP-Ti20%, and CAP#30 bulks at $T_s = 20$ K and, for comparison, those for the GdBaCuO bulk, which is assumed to perform PFM at $T_s = 40$ K.

The l_m values, which indicate the thermal stability of superconductors, are varied for the MgB_2 bulks, which are from twice to one order of magnitude larger than that of the GdBaCuO bulk. In this sense, the thermal stability of the MgB_2 bulk appears to be better than GdBaCuO bulks. However, from the comparison of the specific heat C, the MgB_2 bulk is unstable because the transfer energy to the normal state for the MgB_2 bulk is one twentieth smaller than that of the GdBaCuO bulk at each T_s. The d_c values, which indicate the magnetic stability of superconductors, decreases with increasing J_c values of the bulk and are also smaller than that of the GdBaCuO bulk. In any case, the thermal and magnetic stability decreases for the MgB_2 bulk, compared with that for the GdBaCuO bulk at each T_s. The discussion using the l_m and d_c values is based on the heat flow in one dimension rather than the three dimensions in the case of a bulk, which is therefore only a first approximation. The detailed analysis remains to understand the thermal and magnetic stability in the MgB_2 bulk during PFM.

IV. CONCLUSION

We have performed the pulsed-field magnetization (PFM) for MgB_2 superconducting bulks with higher critical current density $J_c(B)$. During PFM, a flux jump took place frequently and the trapped field B_z decreased in the disk-shaped bulks for higher applied magnetic field. However, in the cylindrical bulk with identical $J_c(B)$ characteristics, the flux jump was avoided. The maximum trapped field of $B_z = 0.81$ T was obtained at 14 K, which is a record-high trapped field in an MgB_2 bulk by PFM. The key solution may include in an optional aspect ratio (d/t_B) of the bulk to avoid the flux jumps during PFM. The electromagnetic and thermal stability was discussed using the parameters of minimum propagation zone (MPZ) l_m and critical thickness d_c, suggesting that MgB_2 bulks with higher $J_c(B)$ are unstable, compared with the GdBaCuO bulk.

REFERENCES

[1] M. Murakami, "Processing and Applications of Bulk RE-Ba-Cu-O Superconductors," *Int. J. Appl. Ceramic Technol.*, vol. 4, no. 3, pp. 225–241, Jul. 2007.

[2] M. Kambara *et al.*, "High intergranular critical currents in metallic MgB_2 superconductor," *Supercond. Sci. Technol.*, vol. 14, no. 4, pp. L5–L8, Apr. 2001.

[3] A. Yamamoto *et al.*, "Development of MgB_2 bulk superconducting magnet," in *Proc. Abstract 23rd Int. Symp. Supercond.*, 2010, pp. 219–219.

[4] J. H. Durrell *et al.*, "A trapped field of > 3 T in bulk MgB2 fabricated by uniaxial hot pressing," *Supercond. Sci. Technol.*, vol. 25, no. 11, Nov. 2012, Art. ID. 112002.

[5] T. Naito, T. Yoshida, and H. Fujishiro, "Realization of 4.6 T trapped field in double stacked MgB_2 bulk pair by Ti-doping," *Supercond. Sci. Technol.*, to be published.

[6] G. Fuchs *et al.*, "High trapped fields in bulk MgB_2 prepared by hot-pressing of ball-milling precursor powder," *Supercond. Sci. Technol.*, vol. 26, no. 12, Dec. 2013, Art. ID. 122002.

[7] Y. Yanagi *et al.*, "Trapped field distribution on Sm-Ba-Cu-O bulk superconductor by pulsed-field magnetization," in *Advances in Superconductivity XII*. Tokyo, Japan: Springer-Verlag, 2000, pp. 470–473.

[8] M. Sander, U. Sutter, R. Koch, and M. Klaser, "Pulsed magnetization of HTS bulk parts at $T < 77$ K," *Supercond. Sci. Technol.*, vol. 13, no. 6, pp. 841–845, Jun. 2000.

[9] M. D. Ainslie *et al.*, "Modelling and comparison of trapped fields in (RE)BCO bulk superconductors for activation using pulsed field magnetization," *Supercond. Sci. Technol.*, vol. 27, no. 6, Jun. 2014, Art. ID. 065008.

[10] H. Fujishiro, T. Tateiwa, A. Fujiwara, T. Oka, and H. Hayashi, "Higher trapped field over 5 T on HTSC bulk by modified pulsed field magnetizing," *Physica C*, vol. 445–448, pp. 334–338, Oct. 2006.

[11] H. Fujishiro, T. Naito, T. Ujiie, A. Figini Albisetti, and G. Giunchi, "Trapped field and flux dynamics in MgB_2 superconducting bulks magnetized by pulsed field," *Physics Procedia*, to be published.

[12] H. Fujishiro *et al.*, "Numerical simulation of trapped field and temperature rise in MgB_2 bulks magnetized by pulsed field," *IEEE Trans. Appl. Supercond.*, vol. 23, no. 3, Jun. 2013, Art. ID. 6800804.

[13] T. Naito, T. Sasaki, and H. Fujishiro, "Trapped magnetic field and vortex pinning properties of MgB_2 superconducting bulk fabricated by a capsule method," *Supercond. Sci. Technol.*, vol. 25, no. 9, Sep. 2012, Art. ID. 095012.

[14] T. Sasaki, T. Naito, and H. Fujishiro, "Trapped field and critical current density of MgB_2 bulk fabricated by a capsule method," in *Proc. ICEC-ICMC*, 2013, pp. 875–878.

[15] C. P. Bean, "Magnetization of hard superconductors," *Phys. Rev. Lett.*, vol. 8, pp. 250–253, 1962.

[16] H. Fujishiro, T. Naito, and T. Yoshida, "Numerical simulation of the trapped field in MgB_2 bulk disks magnetized by field cooling," *Supercond. Sci. Technol.*, vol. 27, no. 6, Jun. 2014, Art. ID. 065019.

[17] M. N. Wilson, *Superconducting Magnets*. Oxford, U.K.: Clarendon, 1983.